
Analytical model for geometrical characteristics control of laser sintered surfaces

Y. Ioannou and C. Doumanidis

Department of Mechanical Engineering,
University of Cyprus,
75 Kallipoleos Ave., 1678 Nicosia, Cyprus
E-mail: ioannouy@gmail.com
E-mail: cdoumani@ucy.ac.cy

M.M. Fyrillas

Department of Mechanical Engineering,
Frederick University,
Y. Frederickou Str., 1303 Nicosia, Cyprus
Fax: +357 22 438234
E-mail: m.fyrillas@frederick.ac.cy
E-mail: m.fyrillas@gmail.com

K. Polychronopoulou*

Department of Mechanical Engineering
and
Department of Chemistry,
University of Cyprus,
75 Kallipoleos Ave., 1678 Nicosia, Cyprus
E-mail: kyriakip@ucy.ac.cy
*Corresponding author

Abstract: Selective laser sintering (SLS) is an additive rapid manufacturing technique where a high-power laser is used to fuse micro- and nano-particles into a specified three-dimensional geometry. The goal of this work was to develop an analytical model for the SLS manufacturing process in order to control the geometrical characteristics of the sintered areas when iron/copper (Fe/Cu) powder alloy is used on a flat substrate. Powder particles are subject to melting by the laser energy and form a liquid globule that solidifies as the laser beam spot moves along the substrate. The model is developed by considering lumped mass and energy balances and fluid dynamic equilibrium of the sintered material. It is assumed that the process is two-dimensional and axisymmetric. It is further assumed that the energy delivered by the laser is used to sinter the material rising its temperature up the melting point, while the energy lost due to conduction in the metal substrate is very small. The sintered area geometry is parameterised and the parameters are obtained by solving a system of nonlinear algebraic equations.

Keywords: laser sintering; geometrical characteristics modelling; heat transfer; metal powder; surface tension.

Reference to this paper should be made as follows: Ioannou, Y., Doumanidis, C., Fyrillas, M.M. and Polychronopoulou, K. (2010) 'Analytical model for geometrical characteristics control of laser sintered surfaces', *Int. J. Nanomanufacturing*, Vol. 6, Nos. 1/2/3/4, pp.300–311.

Biographical notes: Yiannos Ioannou received his BSc from the University of Patras (Greece, 2007) in Mechanical Engineering and Aeronautics. Currently, he is a PhD Researcher at the Mechanical and Manufacturing Engineering Department of the University of Cyprus. His research interests include nanomanufacturing, thermal manufacturing, materials and surface characterisation and modelling.

Charalabos Doumanidis (PhD, MIT, 1988) is Marie Curie Chair and Interim Director of Hephaistos Nanotechnology Research Center at the University of Cyprus (2003–present). His research interests include nanoscale manufacturing, thermal processing of materials, deposition and joining processes, rapid prototyping, rapid thermal processing of semiconductors, distributed parameter system modelling and control, robotics and mechatronics and biomedical instrumentation. He is the author of over 180 refereed papers (including three best paper awards), seven patents and two book chapters. He is a recipient of the EC Marie Curie Chair (2004), ASME Blackall Award (2002), White House Presidential Faculty Fellow Award (1996), etc.

Marios M. Fyrillas is an Associate Professor of Mechanical Engineering at Frederick University, Cyprus. His research work deals with fundamental problems in theoretical fluid dynamics and transport phenomena, and has been motivated by a wide spectrum of topics such as chemical processes, manufacturing, crowd simulation (<http://staff.fit.ac.cy/eng.fm/>). He received his PhD from the University of California, Irvine.

Kyriaki Polychronopoulou received her BSc in Chemistry (2000) from the University of Cyprus (UCY) and her PhD in Chemistry with strong emphasis in heterogeneous (environmental) catalysis in 2005 (UCY). She has also received an MSc in Mechanical Engineering with focus in surface engineering (UCY, 2008). As a Postdoctoral Researcher, she worked at the Technical University of Leoben (Austria, 2006), at the University of Surrey (UK, 2006) and at the University of Illinois at Urbana-Champaign (IL, USA, 2007). She had academic appointments as a Visiting Lecturer at the Department of Mechanical and Manufacturing Engineering (UCY, 2006) and Chemistry Department (UCY, 2008).

1 Introduction

Selective laser sintering (SLS) offers unique advantages over conventional thermo-mechanical processes, and for this reason it is one of the leading commercial rapid prototyping processes used so far. The process involves formation of fabricating solid objects by selectively fusing powder of successive layers according to numerically defined cross-sectional geometry. Some successful results have been obtained with different powder mixtures, such as Fe-Cu, WC-Co, TiC-Ni/Co/Mo, TiCN-Ni, TiB₂-Ni, ZrB₂-Cu and Fe₃C-Fe, each containing two metal powders and fusing only the powder having the lower melting point (Zhu et al., 2003; Wang et al., 2002). Several physical

phenomena are involved in the SLS process. Heat generation and transfer (the heating of the powder bed and the cooling of the sintered sample); microstructure evolution (porosity evolution and phase changes); fluid effects (molten binder flowing in the solid consolidate) and mechanical issues (non-uniform distribution of thermal strains during the cooling stage may cause residual stresses and distortions of parts produced) (Zhu et al., 2003). In these coexisting physical phenomena, thermal effects are dominant (German, 1985). Other mechanical and fluidic aspects, caused directly or indirectly by this thermal process, occur at different processing stages. It is clear from the above that knowing the temperature distribution and evolution is essential to understand the SLS process.

Sintering takes place if the powder bed is irradiated by the moving laser source up to the temperature at which the binder phase melts. After the laser has moved away, the sintered sample cools down. The thermal process in SLS may be summarised in four main stages: energy input and absorption, heating of the powder bed, binder melting and sintering, and cooling of the sintered sample.

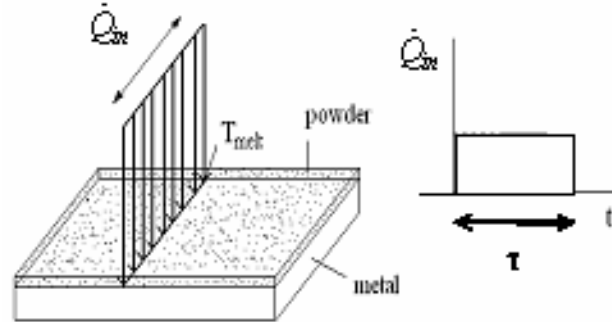
Fe-Cu is a well-described material system for liquid-phase sintering (LPS) because this material system has good surface wetting. Because the reflectivity of Cu is higher than that of Fe, the SLS of Fe-Cu requires careful control of grain size and mixing ratio of the powders to avoid melting of Fe before Cu. It is an ideal metallurgy material utilised for fabricating tooling because of its good mechanical properties: the hard Fe lattice is dispersed in a ductile Cu matrix. Moreover, the price of these two powders is relatively low.

2 Mathematical modelling

2.1 Experimental procedure

SLS process and physical description: The material to be sintered consists of a mixture of two powders: a high-melting-point powder, called the structural powder, and a powder having a lower melting point, called the binder (Cu). This mixture is spread as a thin layer, normally 0.1–0.5 mm in thickness. The mixed powders are then heated by a rapidly scanning laser beam to the temperature at which the binder melts. Another important characteristic is that the sintering time is short in SLS, because the scanning laser beam supplies energy to each cross-sectional location only for about 1 ms–0.1 s. Once the binder is molten and has flown into the pores between the unmolten structural particles, the system cools down. No further densification can take place in such a short time interval.

Localised heating of small volumes of powder during SLS is shown schematically in Figure 1. The five independent process parameters that are most influential in governing the intensity and method of the energy delivered to the powder surface are: laser power \dot{Q}_{in} , laser beam distribution spot size (i.e., width of heated zone), laser equivalent velocity v , hatch spacing (i.e., distance between adjacent laser scans) and scan line length L . Phenomena such as wettability, viscosity and flow play an important role to the metallurgical process. In the nomenclature all the parameters of the model are listed.

Figure 1 Interaction of laser irradiation with metal powder

Note: A laser beam with power \dot{Q}_{in} , delivers an amount of energy $Q_{in} = \dot{Q}_{in}\tau$ to the scanned powder segment.

2.2 Theoretical model

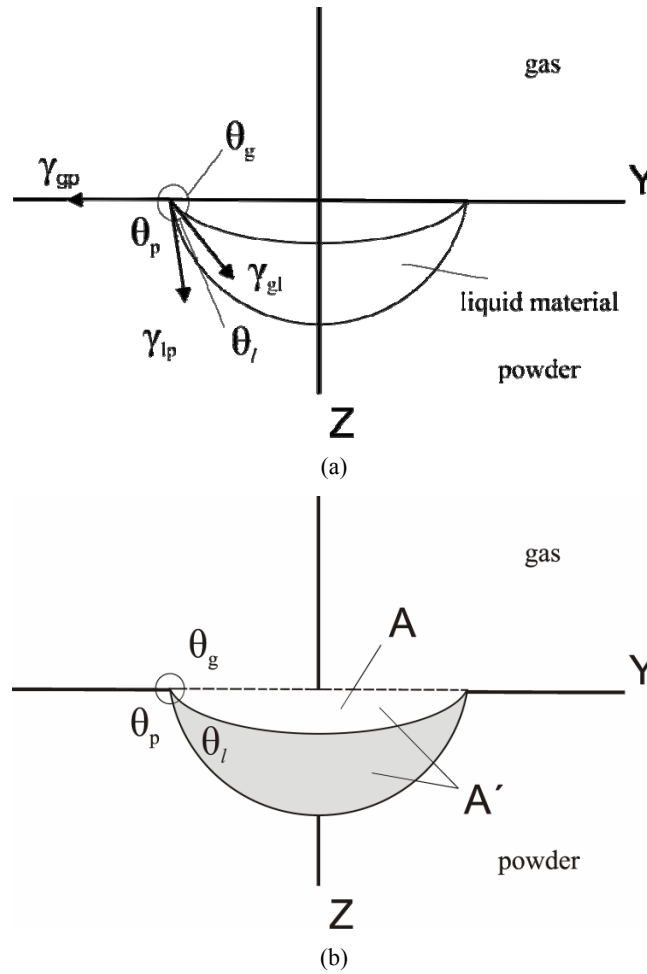
As mentioned, in the previous section, the sintering process is achieved by a scanning laser beam, moving along the span of the scanned segment with velocity v , delivering an amount of energy to the powder-bed. The energy is conducted first through the powder, which is assumed to be a continuum medium, and then through the metal-substrate. In view of the small distribution spot size SP of the laser beam, the energy delivery process is modelled as a point source delivering a constant power \dot{Q}_{in} . In view of the rapid movement of the point source, we can further assume that the power of the laser beam is distributed simultaneously and evenly along the span of the scanned segment of the powder-bed for a time period $\tau = L/v$, where L is the span of the powder-bed (Figure 1), delivering a total energy of $Q_{in} = \dot{Q}_{in}\tau$ (Figure 1). The net energy delivered per unit length is defined as $q_{in} = Q_{in}/L = \dot{Q}/v$, and this is assumed to be injected uniformly over the time τ . As the heat is conducted through, a phase-change takes place. In particular, an interface surface is developed with temperature T_{melt} that separates the sintered material (liquid) from the solid material (powder and metal). Because of the assumed thermal uniformity (due to the fast laser scanning) along the segment length, the uniform temperature distribution along the segment yields a uniform cross-sectional profile of the solid-melt interface (except possibly at its very edges).

The interface travels across the cross-section through the powder-layer and metal-substrate and its path determines the final profile of the sintered material. The objective of this work is to determine this profile. The problem is considered to be a two-stage process. Taking a cross section on the first stage, the solid-liquid interface has not yet reached the metal substrate. Immediately after the interface reaches the metal substrate the second stage of the process begins. By applying mass and energy conservation, and assuming that the contact angles of the three-phase contact lines associated with the two interfaces are known, we develop a system of algebraic equations through which the parameters of the profile can be obtained. The symbols used are all listed in the nomenclature.

2.2.1 Initial stage

The model is developed by considering mass conservation, energy balance and fluid dynamic equilibrium of the sintered material on each phase. Through preliminary experimental evidence, provided by MANUDIRECT project partner, the interfaces between the gas/liquid and the liquid/powder material are assumed to take the shape of circular arcs.

Figure 2 Meniscus forming as the melted material interface traveling through the powder layer



Mechanical equilibrium

Taking mechanical equilibrium on the y-axis we deduce the following relations (Figure 2b).

$$\gamma_{gp} = \gamma_{lp} \cos(\pi - \theta_p) + \gamma_{gl} \cos(\pi - \theta_p - \theta_l) \tag{1}$$

$$\theta_g + \theta_l + \theta_p = 2\pi \tag{2}$$

Mass balance

The mass of the powder sintered which is associated with the area A' must be equal to the mass of the molten metal occupying the area $(A'-A)$ (Figure 2b).

$$\rho_p A' L = \rho_m (A' - A) L \quad (3)$$

Energy balance

If the heat losses to the environment by radiation and convection are negligible compared to conduction losses to the substrate (q_p) and the energy absorbed for sintering (q_{melt}), then the latter has two components: The energy required in order to increase the internal energy of the material to T_{melt} and the latent heat required to melt it. By applying the energy conservation on the two-dimensional profile we have.

$$q_m = q_p + q_{melt} \quad (4)$$

$$q_{melt} = \rho_m \Delta H (A' - A) + \rho_m C_p A' (T_{melt} - T_o) \quad (5)$$

where q_p is the heat transferred due to conduction in the powder and it is assumed to obey 1-d transient heat conduction.

$$q_p = \frac{K_p \Delta T}{(\pi \alpha)^{1/2}} C \sqrt{t} \quad (6)$$

where ΔT is the temperature difference $T_{melt} - T_o$, C is circumference (Figure 3) and t is the time elapsed since the start of the process.

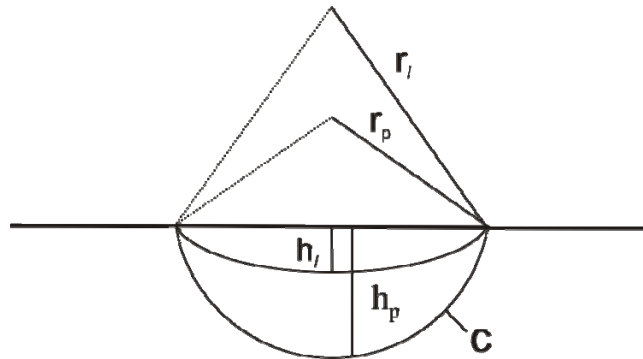
Geometrical relations

The geometrical relations required for the first-stage are:

$$A' = r_p^2 \cos^{-1} \frac{r_p + h_p}{r_p} - (r_p - h_p) \sqrt{2r_p h_p - h_p^2} \quad (7)$$

$$A = r_l^2 \cos^{-1} \frac{r_l + h_l}{r_l} - (r_l + h_l) \sqrt{2r_l h_l - h_l^2} \quad (8)$$

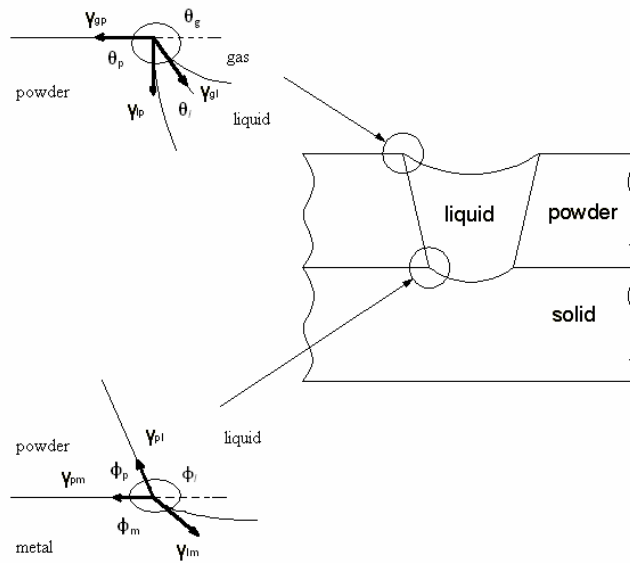
Figure 3 Geometrical parameters for the first stage



2.2.2 Second stage and equilibrium shape of the final profile

In order to determine the final profile of the sintered material, we assume a shape for each segment of the profile. In particular: a. in view of the small thickness of the powder-layer compared to the width of the sintered zone, the side segments, which are interfaces between the powder and the liquid melted material, are assumed to be straight (Figure 4) b. the top and bottom segments, which are interfaces between the gas/liquid and the liquid/substrate metal (Figures 3–4) respectively, are assumed to take the shape of circular arcs of circles (as suggested by preliminary experimental micrographs).

Figure 4 Equilibrium at the line of contact of three different media



This is justified in view of the fact that a circular arc is an asymptotic solution to the Laplace-Young equation. The Laplace-Young equation describes the shape of a curved interface with uniform tension γ separating two stationary fluids. The boundary conditions of the Laplace-Young equation are dictated from the contact angles of the triple points, i.e., liquid/powder/gas and solid/powder/liquid material systems. These assume horizontal mobility of the triple points (because of the liquid and powder phases), and depend only on the materials and in no other way on the conditions of the problem (Batchelor, 1967).

Mechanical equilibrium

The contact angles can be deduced from an independent experiment using equilibrium on the horizontal axis for the contact lines along the three media (Figure 4):

$$\gamma_{gp} = \gamma_{lp} \cos(\pi - \theta_p) + \gamma_{gl} \cos(\pi - \theta_p - \theta_l) \tag{9}$$

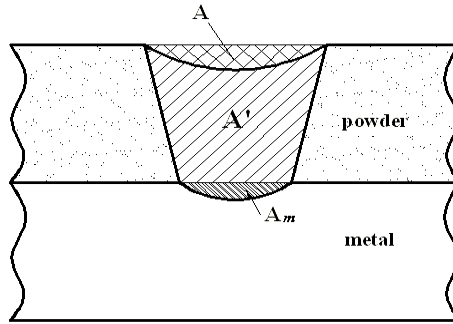
$$\gamma_{pm} + \gamma_{lp} \cos(\varphi_p) = \gamma_{ml} \cos(\pi - \varphi_m) \tag{10}$$

Mass balance

Mass conservation of the molten material suggests that the mass of the powder sintered, which is associated with the trapezoid with area $(A + A')$, must be equal to the mass of the molten metal occupying the area A' :

$$\rho_m A' L = \rho_p (A + A') L \quad (11)$$

Figure 5 Geometry areas A and A' used in the mass balance



Here, we have assumed that the density of the molten material is nearly equal to the density of the solid metal. The areas A and A' are shown clearly in Figure 5 and the parameters involved are identified in the previous section.

Energy balance

Applying the energy conservation (Incropera and DeWitt, 1996) per unit length on the two-dimensional profile (Figure 5), we obtain the following equation:

$$q_m = q_p + q_m + q_{melt} \quad (12)$$

where q_m is the energy input from the laser, and q_p and q_m denote the energy transferred due to heat conduction in the powder and the metal-substrate respectively:

$$q_p = \frac{K_p \Delta T}{\sqrt{\pi \alpha_p}} 2l_p \sqrt{t} \quad (13)$$

The parameter l_p is the cross-sectional of the interface between the powder and the melted material, which is assumed to be straight linear segment. Similar to q_p , q_m is estimated assuming 1-D transient heat conduction problem, where t is the time.

$$q_m = \frac{K_m \Delta T}{\sqrt{\pi \alpha_m}} c_m \sqrt{t} \quad (14)$$

The energy absorbed for sintering (q_{melt}) has two components. The energy required in order to increase the internal energy of the material to T_{melt} and the latent heat required to melt it:

$$q_{melt} = \rho_m (A' + A_m) \Delta H + \rho_m C_p A' (T_{melt} - T_o) + \rho_m A_m C_m \tag{15}$$

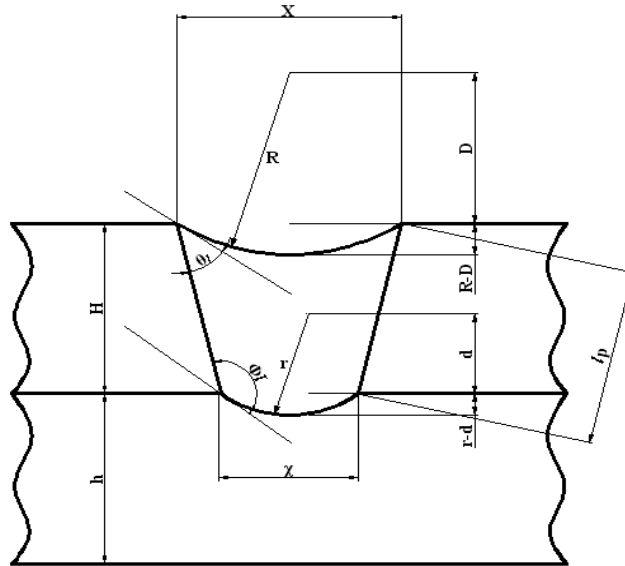
Geometrical relations

Based on the geometrical formulation of the model we deduce the followings trigonometric relations between the contact angles and the geometrical parameters (Figure 6):

$$\tan^{-1} \left(\frac{H}{(X-x)/2} \right) - \left(\frac{\pi}{2} - \cos^{-1} \frac{x/L}{2} \right) = \theta_l \tag{16}$$

$$\left(\pi - \tan^{-1} \left(\frac{H}{(X-x)/2} \right) - \tan^{-1} \frac{d}{x/2} \right) + \frac{\pi}{2} = \Phi_l \tag{17}$$

Figure 6 Equilibrium at the line of contact of three different media



In what follows, we will also require expressions for the areas associated with each section of the profile. These sections are clearly indicated in Figure 5, and the expressions can be found in CRC (2002):

$$A = R^2 \cos^{-1} \left(\frac{D}{R} \right) - D \sqrt{2R - D^2} \tag{18}$$

$$A' = \frac{X-x}{2} H - A \tag{19}$$

$$A_m = r^2 \cos^{-1} \left(\frac{d}{r} \right) - d \sqrt{2r - d^2} \tag{20}$$

where

$$R = \sqrt{D^2 + (X/2)^2} \quad \text{and} \quad r = \sqrt{d^2 + (x/2)^2} \quad (21)$$

In order to obtain the final profile, it is sufficient to determine the parameters D , d , X and x . These geometric relationships along with the mechanical equilibrium and the mass and energy conservation equations established before, constitute a system of equations for these four unknown parameters defining the sintered profile.

2.3 Numerical results

To find the final profile we assumed that the sintering process terminates at $t = \tau$. This provides us with an estimate of the heat conducted and along with the other parameters it is possible to estimate the final profile. In principle the system of equations (11), (15), (16) and (17) along with (18), (19), (20) and (21) is a consistent system of equations for the four unknown steady-state parameters D , d , X and x . The system of equations is solved numerically using the *fsolve* function of the commercial software Matlab7. The material and experimental properties used have been compiled from the literature (Zhu et al., 2003; Chen and Zhang, 2006):

Table 1 Sintering parameters applied in the numerical simulation

L	0.3 m
H	0.0003 m
w	0.3 m
h	0.01 m
C_p	480 J/K Kg
C_m	450 J/K Kg
ΔH	213,000 J/Kg
q_m	3,000 J/m
τ	0.1 s
θ_l	48 degrees
φ_l	136.5 degrees
ρ_p	7,000 kg/m ³
ρ_m	6,500 kg/m ³

The results obtain are as follows: $X = 0.0005364$ m, $x = 0.0005165$ m, $D = 0.0003184$ m, $d = 0.0002618$ m which correspond to $R = 0.00042$ m and $r = 0.00037$ m. The results are in agreement with experimental results. These results are in the process of being verified experimentally on a Nd:YAG Laser processing station (Rofin Starweld).

3 Conclusions

In this study, a 2-D analytical geometry model for the SLS manufacturing processes is proposed in order to obtain the geometrical characteristics of the sintered area when iron/copper (Fe/Cu) powder alloy is processed on a flat substrate. The energy delivery process is modelled as a line source delivering a spatially uniform, temporally constant power. The objective of the work is to obtain the final profile of the sintered material. The final profile is parameterised by assuming that the side segments are straight, which is justified in view of the small thickness of the powder-layer compared to its width. Furthermore, the top and bottom interfaces, which separate the gas/liquid and liquid/metal-substrate respectively, are assumed to take the shape of circular arcs. We also assume that the energy transfer due to radiative and convective heat losses can be neglected in view of the instant fusion of the powder and the relatively fast solidification of the molten material. By applying mass and energy conservation, and assuming that the contact angles of the three-phase contact lines associated with the two interfaces are known, a system of four static nonlinear algebraic equations is obtained through which the steady-state parameters of the profile can be obtained. The system of the four nonlinear algebraic equations is solved numerically using material and experimental properties from the literature. The results obtained are in the process of being validated through experimental measurements of the shape of the sintered zone.

Acknowledgements

Authors would like to acknowledge EU project MANUDIRECT (Contract No. NMP2-CT-2006-026467) for funding this work and research infrastructure program NANOCYPRUS (ERYNE0504/02) by the Cyprus Research Promoting Foundation (RPF).

References

- Batchelor, G.K. (1967) *An Introduction to Fluid Dynamics*, Cambridge University Press.
- Chen, T. and Zhang, Y. (2006) 'Three-dimensional modeling of selective laser sintering of two-component metal powder layers', *Journal of Manufacturing Science and Engineering*, Vol. 128, pp.299–306.
- CRC (2002) *CRC Standard Mathematical Tables*, 3rd ed., CRC press.
- German, R.M. (1985) *Liquid Phase Sintering*, Plenum Press, New York.
- Incropera, F.P. and DeWitt, D.P. (1996) *Introduction to Heat Transfer*, 3rd ed., Wiley, New York.
- Wang, X.C., Laoui, T., Bonse, J., Kruth, J.P., Lauwers, B. and Froyen, L. (2002) 'Direct selective laser sintering of hard metal powders: Experimental study and simulation', *Int. J. Adv. Manuf. Technol.*, Vol. 19, pp.351–357.
- Zhu, H.H., Fuh, J.Y.H. and Lu, L. (2003) 'Formation of Fe-Cu metal parts using direct laser sintering', *J. Mechanical Engineering Science Proc. Instn. Mech. Engrs.*, Vol. 217, pp.139–147.

Nomenclature

C_p	Thermal capacitance of powder	J/kg K
C_m	Thermal capacitance of metal	J/kg K
D, d	Centre to chord distance	m
ΔH	Latent heat	J/kg
HS	Hatch spacing	m
H	Metal substrate height	m
h	Powder height	m
k_p	Thermal conductivity of the powder	W/m * K
k_m	Thermal conductivity of metal	W/m * K
L	Scan line length	m
\dot{Q}_m	Laser power	W (watt)
q_{in}	Energy delivered by laser	J/m
q_p	Energy due to conduction in the powder per unit length	J/m
q_m	Energy due to conduction in the metal substrate	J/m
R, r	Radius of circle	m
S	Dimensionless shape factor	
SP	Laser spot size	m/s
T_o	Ambient temperature	K
T_{melt}	Powder melting temperature	K
v	Laser velocity	m/s
w	Width of the metal substrate	m
X, x	Chord of circle	m
c	Circumference	
t	Instantaneous time of the solid-liquid interface	s
<i>Greek symbols</i>		
α	Thermal diffusivity	m ² /s
γ	Surface tensions	N/m
τ	Time period	s
ρ_p	Powder density	Kg/m ³
ρ_m	Metal density	Kg/m ³
<i>Subscripts</i>		
g	Gas	
p	Powder	
l	Liquid	
m	Metal	
